SIAM J. IMAGING SCIENCES
Vol. 16, No. 2, pp. 614–639

Stability and Reconstruction of a Special Type of Anisotropic Conductivity in Magneto-Acoustic Tomography with Magnetic Induction*

Niall Donlon†, Romina Gaburro‡, Shari Moskow§, and Isaac Woods§

Abstract. We consider the issues of stability and reconstruction of the electrical anisotropic conductivity of biological tissues in a domain $\Omega \subset \mathbb{R}^3$ by means of the hybrid inverse problem of magneto-acoustic tomography with magnetic induction (MAT-MI). The class of anisotropic conductivities considered here is of type $\sigma(\cdot) = A(\cdot, \gamma(\cdot))$ in Ω, where $[\lambda^{-1}, \lambda] \ni t \mapsto A(\cdot, t)$ is a one-parameter family of matrix-valued functions which are a priori known to be $C^{1,\beta}$, allowing us to stably reconstruct γ in Ω in terms of an internal functional $F(\sigma)$. Our results also extend previous results in MAT-MI where $\sigma(\cdot) = \gamma(\cdot)D(\cdot)$, with D an a priori known matrix-valued function on Ω to a more general anisotropic structure which depends nonlinearly on the scalar function γ to be reconstructed.

Key words. hybrid inverse problems, MAT-MI, anisotropic conductivity, stability, reconstruction

MSC codes. 35R30, 35Q61, 65N21, 78A70

DOI. 10.1137/22M1512260

1. Introduction.

In many physical situations, it is important to determine certain physical properties of the interior of a body that cannot be measured directly. Inverse problems are employed to infer such information from external observations. If one is interested in imaging biological tissue inside the human body, its electrical conductivity distribution can provide valuable information about its state. A recently developed noninvasive imaging modality based on the determination of the electrical conductivity distribution of biological tissue is magnetoacoustic tomography with magnetic induction (MAT-MI).

If a biological conductive body, modelled by a domain $\Omega \subset \mathbb{R}^3$ with smooth boundary $\partial\Omega$, is placed in a static magnetic field $B_0 = (0, 0, 1)$, it starts to emit ultrasound waves that can be measured around the body, i.e., at a series of locations on $\partial\Omega$. To be more precise, to cause an eddy current within the conductive tissue, a pulsed time-dependent magnetic field $B(t)$ is applied to excite the tissue in Ω, which, in turn, emits the ultrasound waves. For the sake

*Received by the editors July 28, 2022; accepted for publication (in revised form) December 7, 2022; published electronically May 12, 2023.
https://doi.org/10.1137/22M1512260
Funding: The work of the first and second authors was supported by Irish Research Council grant GOIPG/2021/527. The work of the second author was also partially supported by Science Foundation Ireland grant 16/RC/3918. The work of the third author was partially supported by National Science Foundation grant DMS-2008441.

†Department of Mathematics and Statistics, University of Limerick, Limerick, V94 T9PX, Ireland (niall.donlon@ul.ie).
‡Department of Mathematics and Statistics, Health Research Institute HRI, CONFIRM, University of Limerick, Limerick, V94 T9PX, Ireland (romina.gaburro@ul.ie).
§Department of Mathematics, Drexel University, Philadelphia, PA 19104 USA (slm84@drexel.edu, iw76@drexel.edu).

of simplicity, we follow the research line already initiated in [8], [37]. The pulsed magnetic field is of the form $B_1 u(t)$, where the vector field B_1 is constant and $u(t)$ is a scalar function representing the time variation. As the magnetic permeability of biological tissue and that of a vacuum are approximately equal, the tissue does not have any noticeable effect on the magnetic field itself. Therefore, only the spatial dependence of the magnetic fields needs to be considered. MAT-MI is an example of *hybrid inverse problems*, which typically combine a high contrast modality with a high resolution one and they typically involve two steps. In the first step, a well-posed problem involving high resolution and low contrast modality is solved from the knowledge of boundary measurements. In the second step, a quantitative reconstruction of the parameters of interest (describing a physical property of the medium in question) is solved by knowledge of a so-called *internal functional* which has been reconstructed during the first step. Hybrid methods are mainly concerned with the solution of the second step (assuming that the first step has been successfully performed). For a review on hybrid imaging modalities, we refer to [11].

The first step in MAT-MI is to retrieve the acoustic source from the measurements around the object in the scalar wave equation. Then, in the second step, MAT-MI reconstructs the distribution of electrical conductivity from acoustic source information (see [8], [37]). This second step is the focus of this paper, where we study, in the MAT-MI experiment, the issues of stability and reconstruction for a special type of anisotropic conductivity σ in terms of internal measurements of the acoustic sources (which are assumed to be known after the first step has been performed) modelled by the internal functional

$$F(\sigma) = \nabla \cdot (\sigma E_\sigma \times B_0) \qquad \text{in} \quad \Omega, \tag{1.1}$$

where E_σ solves the Maxwell's equations

$$\begin{cases} \nabla \times E_\sigma = B_0 & \text{in} \quad \Omega, \\ \nabla \cdot \sigma E_\sigma = 0 & \text{on} \quad \Omega, \\ \sigma E_\sigma \cdot \nu = 0 & \text{on} \quad \partial\Omega \end{cases} \tag{1.2}$$

and $\sigma \in C^{1,\beta}(\overline{\Omega})$ is symmetric on Ω and satisfies a uniform ellipticity condition (the precise formulation of the problem is given in section 2).

For clinical and research purposes, the electrical conductivity of biological tissues can provide valuable information as the conductivity varies significantly within the human body. Other and more established medical imaging modalities, like computerized tomography (CT), magnetic resonance imaging (MRI), and ultrasound imaging, are typically capable of creating images of the human body with very high resolution. These modalities often fail to exhibit a sufficient contrast between different types of tissues. Imaging modalities like optical tomography (OT) and electrical impedance tomography (EIT) do, on the other hand, display such high contrast at the expense of a poor resolution (see [9], [13], [41]). EIT, similarly to MAT-MI, also provides information about materials and biological tissues in terms of their conductivity. The resulting images from measurements of electrostatic voltages and current flux taken on the surface of the body under investigatio, are often blurred, due to the EIT poor resolution. MAT-MI, on the other hand, has the potential to overcome this issue by providing images of the conductivity of a body in terms of internal measurements that have

been obtained by means of a high resolution imaging modality performed in the first step of MAT-MI. Hence MAT-MI has the potential to provide high contrast images of a body in terms of its internal conductivity that also benefits from a reasonably good resolution.

Biological tissues are known to have anisotropic conductivity [31]. In EIT, since its first mathematical formulation by Calderón in his 1980 seminal paper [16], a lot of progress has been made, but the problem of uniquely determining the anisotropic conductivity of a body by means of EIT measurements is still considered an open problem. Partial results of uniqueness and stability for this inverse problem have been obtained in [1], [2], [3], [4], [5], [6], [10], [12], [18], [19], [20] [21], [28], [33], [34], [35], [36], [39].

In the MAT-MI experiment, results of stability and reconstruction of the conductivity σ in terms of the internal functional $F(\sigma)$ given in (1.1), have been obtained in [37] and [8], where the isotropic case $\sigma = \gamma I$ (here I denotes the 3×3 identity matrix and γ is a positive scalar function on Ω) and the special anisotropic case $\sigma = \gamma D$, with D a known 3×3 symmetric matrix and γ is a positive scalar function on Ω, were considered, respectively. In the present paper, we extend these results to the case where the anisotropic conductivity σ is of type $\sigma = A(\cdot, \gamma(\cdot))$, and $A(\cdot, t)$ is known for $t \in [\lambda^{-1}, \lambda]$.

More precisely, we start by considering the simpler case where σ is a symmetric, uniformly positive definite matrix which is a priori known to have the structure $\sigma(x) = A(\gamma(x))$, $x \in \overline{\Omega}$, where the one-parameter family of matrix-valued functions

$$t \mapsto A(t), \qquad t \in [\lambda^{-1}, \lambda]$$

is assumed to be known and to belong to a certain class $\mathcal{A}$ defined below (Definition 2.2) and $\gamma = \gamma(x)$, $x \in \overline{\Omega}$ is an unknown scalar function to be determined. The above structure for σ is also generalized to the case $\sigma = A(x, \gamma(x))$, $x \in \overline{\Omega}$, where the one-parameter family of matrix-valued functions

$$t \mapsto A(x, t) \qquad \text{for any} \quad x \in \overline{\Omega}, \qquad t \in [\lambda^{-1}, \lambda]$$

is assumed to be known and to belong to a certain class $\mathcal{A}'$ defined below (Definition 2.5) and $\gamma = \gamma(x)$, $x \in \overline{\Omega}$ is again an unknown scalar function to be determined. The latter, in particular, extends the results in [37] and [8], where the problem of stability and reconstruction in MAT-MI has been addressed in the isotropic case and in the anisotropic case $\sigma(x) = \gamma(x)D(x)$, where D, in this case, is a known matrix-valued function and $\gamma = \gamma(x)$, $x \in \overline{\Omega}$ is the unknown scalar function to be determined. For both cases when $A \in \mathcal{A}$ and $A \in \mathcal{A}'$ considered in this manuscript, we prove that we can stably reconstruct the scalar function γ in terms of F.

In this paper we also present several numerical experiments in which we reconstruct the scalar function $\gamma = \gamma(x)$, $x \in \Omega$ for both types of anisotropic conductivities $\sigma(x) = A(\gamma(x))$ and $\sigma(x) = A(x, \gamma(x))$, $x \in \Omega$. We start by considering a number of examples in which $A \in \mathcal{A}$ only (Examples 1–4). The more general case of $A \in \mathcal{A}'$ is exploited in Examples 5 and 6. The reconstruction is based on an algorithm introduced in [37], [8], which relies on projecting its iterates into a convex subset of $C^{1,\beta}(\Omega)$ in order to restore well posedness in the inverse problem. We note that in the particular examples considered here, the projection step seems unnecessary for the convergence of the iterates. Moreover, in two of our examples,

the true conductivity γ_* we wish to reconstruct is not C^1, hence is less regular than the classes of conductivities we considered in our theoretical framework. This not only allows us to test the performance of the reconstruction algorithm on nonsmooth data, but it also provides insights about possibly lowering the regularity of the conductivity considered in our theoretical framework (the stability estimates in section 2 and the convergence analysis we carry out in subsection 4.2). It will be part of future work to extend our theoretical framework to a class of conductivities with lower regularity assumptions and a more general anisotropic structure. The anisotropic structures considered in the current paper are one-parameter families of symmetric and uniformly positive definite matrices that depend on the unknown scalar function γ in a nonlinear way, extending the results in [8] to the case of a more realistic dependence of the anisotropic structure on the unknown scalar function γ. If, for example, γ was representing the temperature of Ω, then the dependence of A on γ might not be linear. We wish to stress that this paper aims at providing a first step in the treatment in MAT-MI of anisotropic structures that depend nonlinearly on (possibly) a finite number of unknown scalar functions to be stably reconstructed in the MAT-MI experiment. It will be the subject of future work to consider the fully anisotropic case and to which extent the MAT-MI experiment can be employed to determine the anisotropic structure itself.

This paper is organized as follows. In section 2 we introduce notation, state our main assumptions, and define precisely the two classes $\mathcal{A}$ and $\mathcal{A}'$ for A, corresponding to both the simpler and spatially dependent anisotropic case, respectively. The main stability results are also contained in this section. Section 3 contains the proofs of our main stability results and includes estimates for the electromagnetic boundary value problem. In section 4 we describe the reconstruction algorithm (subsection 4.1) and prove convergence results (subsection 4.2), again corresponding to both classes of A. Section 5 contains several numerical experiments demonstrating accurate reconstructions, including two cases of nonsmooth true scalar functions γ_* and one fully three dimensional reconstruction. Some final concluding remarks are included in section 7.

2. Main assumptions and stability estimates.

Throughout this paper the medium to be imaged is a bounded domain Ω in $\mathbb{R}^3$ with $C^{1,\beta}$ boundary $\partial\Omega$ (see Definition 2.1), diameter $\operatorname{diam}(\Omega) = M$, for some constant $M > 0$, and Lebesgue measure $\mu(\Omega)$. For a point $x \in \mathbb{R}^3$, we will denote $x = (x', x_3)$, where $x' \in \mathbb{R}^2$ and $x_3 \in \mathbb{R}$. We will also denote by B_r, B'_r the open balls $B_r(0)$ and $B'_r(0)$ in $\mathbb{R}^3$ and $\mathbb{R}^2$, respectively, and by Q_r the cylinder $Q_r(0)$ in $\mathbb{R}^3$ defined by

$$Q_r(0) = B'_r \times (-r, r).$$

From here onwards we fix a number β satisfying $0 < \beta \leq 1$.

Definition 2.1. *Given a bounded domain $\Omega \subset \mathbb{R}^3$, we say that $\partial\Omega$ is of class $C^{1,\beta}$ with constants $r_0, L > 0$ if for every $P \in \partial\Omega$, there exists a rigid transformation of coordinates under which $P = 0$ and*

$$\Omega \cap Q_{r_0} = \left\{ (x', x_3) \in Q_{r_0} \quad | \quad x_3 > \varphi(x') \right\},$$

where φ is a $C^{1,\beta}$ function on B'_{r_0} satisfying

$$\varphi(0) = |\nabla\varphi(0)| = 0$$

and

$$||\varphi||_{C^{1,\beta}(B'_{r_0})} \leq Lr_0,$$

where we use the normalization convention

$$||\varphi||_{C^{1,\beta}(B'_{r_0})} = ||\varphi||_{L^\infty(B'_{r_0})} + r_0||\nabla\varphi||_{L^\infty(B'_{r_0})} + r_0^{1+\beta} \sup_{x',y'\in B'_{r_0},\, x'\neq y'} \frac{|\nabla\varphi(x') - \nabla\varphi(y')|}{|x'-y'|^\beta}.$$

Once and for all it is understood that $\Omega \subset \mathbb{R}^3$ is a bounded domain with diameter $\mathrm{diam}(\Omega) = M$ and $C^{1,\beta}$ boundary $\partial\Omega$. We define below the two classes of admissible anisotropic structures considered in this paper.

Definition 2.2. *Given Λ, $\mathcal{E}_1 > 0$ and denoting by Sym the class of 3×3 real-valued symmetric matrices, we say that $A(\cdot) \in \mathcal{A}$ if the following conditions hold:*

$$A \in C^{1,\beta}([\lambda^{-1},\lambda], Sym), \tag{2.1}$$

$$\sup_{t\in[\lambda^{-1},\lambda]} \left|\frac{dA}{dt}(t)\right| + \sup_{\substack{t_1,\,t_2\in[\lambda^{-1},\lambda]\\ t_1\neq t_2}} \frac{|\frac{dA}{dt}(t_1) - \frac{dA}{dt}(t_2)|}{|t_1-t_2|^\beta} \leq \mathcal{E}_1 \tag{2.2}$$

and

$$\Lambda^{-1}|\xi|^2 \leq A(t)\xi\cdot\xi \leq \Lambda|\xi|^2 \quad \textit{for every} \quad t\in[\lambda^{-1},\lambda], \quad \xi\in\mathbb{R}^3. \tag{2.3}$$

Proposition 2.3. *If $A\in\mathcal{A}$ and γ satisfies*

$$\lambda^{-1} \leq \gamma(x) \leq \lambda \quad \textit{for almost every} \quad x\in\Omega, \tag{2.4}$$

$$||\gamma||_{C^{1,\beta}(\bar\Omega)} \leq K, \tag{2.5}$$

for some constants $\lambda, K > 0$, then we have

$$A(\gamma(\cdot)) \in C^{1,\beta}(\bar\Omega, Sym), \tag{2.6}$$

and furthermore,

$$||A(\gamma(\cdot))||_{C^{1,\beta}(\bar\Omega)} \leq \Lambda + K\mathcal{E}_1 M(1+2M^\beta) := \mathcal{F}_1, \tag{2.7}$$

where M, $\mathcal{E}_1$, and Λ have been introduced above.

Remark 2.4. Note that in Proposition 2.3, as the L^∞ bound λ on γ is absorbed by the $C^{1,\beta}$ bound K on γ, λ does not appear explicitly in the expression for $\mathcal{F}_1$ in (2.7). As $[\lambda^{-1},\lambda]$ is the interval of variability of t, we find it convenient to distinguish in Proposition 2.3 and in what follows, λ from K. It is understood that such distinction will be kept through this entire manuscript.

Proof. The proof is a straightforward consequence of equality

$$
\begin{aligned}
||A(\gamma(\cdot))||_{C^{1,\beta}(\bar{\Omega})} &= ||A(\gamma(\cdot))||_{L^\infty(\bar{\Omega})} \\
&+ M \sup_{1\le i\le 3} \left|\left| \frac{\partial A}{\partial x_i}(\gamma(\cdot)) \right|\right|_{L^\infty(\bar{\Omega})} \\
&+ M^{1+\beta} \sup_{1\le i\le 3} \sup_{\substack{x,y\in\bar{\Omega}\\ x\neq y}} \frac{|\frac{\partial A}{\partial x_i}(\gamma(x)) - \frac{\partial A}{\partial x_i}(\gamma(y))|}{|x-y|^\beta}
\end{aligned} \tag{2.8}
$$

and our assumptions. ∎

Definition 2.5. *Given Λ, $\mathcal{E}_2 > 0$, we say that $A(\cdot,\cdot) \in \mathcal{A}'$ if the following conditions hold:*

$$
A \in C^{1,\beta}(\bar{\Omega} \times [\lambda^{-1}, \lambda], Sym), \tag{2.9}
$$

(2.10)

$$
\begin{aligned}
&\sup_{t\in[\lambda^{-1},\lambda]} \left\{ \sup_{1\le i\le 3} \left|\left| \frac{\partial A}{\partial x_i}(\cdot,t) \right|\right|_{L^\infty(\bar{\Omega})} + \left|\left| \frac{\partial A}{\partial t}(\cdot,t) \right|\right|_{L^\infty(\bar{\Omega})} \right. \\
&+ \sup_{1\le i\le 3} \sup_{\substack{x,y\in\bar{\Omega}\\ x\neq y}} \frac{|\frac{\partial A}{\partial x_i}(x,t) - \frac{\partial A}{\partial x_i}(y,t)|}{|x-y|^\beta} + \sup_{\substack{x,y\in\bar{\Omega}\\ x\neq y}} \frac{|\frac{\partial A}{\partial t}(x,t) - \frac{\partial A}{\partial t}(y,t)|}{|x-y|^\beta} \Big\} \\
&+ \sup_{1\le i\le 3} \sup_{\substack{t_1,t_2\in[\lambda^{-1},\lambda]\\ t_1\neq t_2}} \left\{ \frac{||\frac{\partial A}{\partial x_i}(\cdot,t_1) - \frac{\partial A}{\partial x_i}(\cdot,t_2)||_{L^\infty(\bar{\Omega})}}{|t_1-t_2|^\beta} + \frac{||\frac{\partial A}{\partial t}(\cdot,t_1) - \frac{\partial A}{\partial t}(\cdot,t_2)||_{L^\infty(\bar{\Omega})}}{|t_1-t_2|^\beta} \right\} \le \mathcal{E}_2
\end{aligned}
$$

and

$$
\Lambda^{-1}|\xi|^2 \le A(x,t)\xi\cdot\xi \le \Lambda|\xi|^2 \quad \text{for a.e. } x\in\bar{\Omega} \quad \forall t\in[\lambda^{-1},\lambda], \quad \forall \xi\in\mathbb{R}^3. \tag{2.11}
$$

We observe that (2.3), (2.11) are conditions of uniform ellipticity.

Proposition 2.6. *If $A \in \mathcal{A}'$ and γ satisfies (2.4), (2.5), then we have*

$$
||A(\cdot,\gamma(\cdot))||_{C^{1,\beta}(\bar{\Omega})} \le \Lambda + M\mathcal{E}_2(1+K)(1+M^\beta(2+K^\beta)) := \mathcal{F}_2, \tag{2.12}
$$

where M, $\mathcal{E}_2$, and Λ have been introduced above.

Proof. This is a straightforward consequence of equalities

$$
\frac{\partial A}{\partial x_i}(x,\gamma(x)) = \frac{\partial A}{\partial x_i}(x,t)|_{(x,t)=(x,\gamma(x))} + \frac{\partial A}{\partial t}(x,t)|_{(x,t)=(x,\gamma(x))} \frac{\partial \gamma}{\partial x_i}(x), \tag{2.13}
$$

together with our assumptions. ∎

Below are our two stability estimates of γ in terms of the internal functional F for the two classes of admissible anisotropic structures $\mathcal{A}$ and $\mathcal{A}'$, respectively.

Theorem 2.7. *Let $A \in \mathcal{A}$ and assume γ_i satisfies (2.4), (2.5) for $i = 1, 2$, $\gamma_1 = \gamma_2$ on $\partial\Omega$ and*

$$||\nabla(\gamma_1 - \gamma_2)||_{L^2(\Omega)} \leq \mathcal{C}||\gamma_1 - \gamma_2||_{L^2(\Omega)} \tag{2.14}$$

for some constant $\mathcal{C} > 0$. Denoting

$$F_i := \nabla \cdot (A(\gamma_i)E_{A(\gamma_i)} \times B_0) \qquad \text{for} \quad i = 1, 2 \tag{2.15}$$

if $\mathcal{C}\Big(C_1(\mathcal{E}_1 + 1) + \Lambda C_3\Big) < \frac{1}{2}$, where C_1, C_3 are the positive constants appearing in (3.6), (3.7), respectively (with $C_3 = \Lambda\mathcal{E}_1 C_1$), then

$$||\gamma_1 - \gamma_2||_{L^2(\Omega)} \leq C||F_1 - F_2||_{L^2(\Omega)}, \tag{2.16}$$

where $C > 0$ is a constant that depends on $\mathcal{C}$, K, $\mathcal{E}_1$, Λ, M, r_0, L, and $\mu(\Omega)$ only.

More generally, we obtain the following main stability result.

Theorem 2.8. *Let $A \in \mathcal{A}'$ and γ_i be as in Theorem 2.7, for $i = 1, 2$. Denoting*

$$\tilde{F}_i := \nabla \cdot (A(\cdot, \gamma_i)E_{A(\cdot,\gamma_i)} \times B_0) \qquad \text{for} \quad i = 1, 2 \tag{2.17}$$

if $\mathcal{C}\Big(C_2(\mathcal{E}_2 + 1) + \Lambda C_4\Big) < \frac{1}{2}$, where C_2, C_4 are the positive constants appearing in (3.8), (3.9), respectively (with $C_4 = \Lambda\mathcal{E}_2 C_2$), then

$$||\gamma_1 - \gamma_2||_{L^2(\Omega)} \leq \tilde{C}||\tilde{F}_1 - \tilde{F}_2||_{L^2(\Omega)}, \tag{2.18}$$

where $\tilde{C} > 0$ is a constant that depends on $\mathcal{C}$, K, $\mathcal{E}_2$, Λ, M, r_0, L, and $\mu(\Omega)$only.

3. Proof of the stability estimates.

To prove our main stability results, we proceed by reducing the Maxwell system (1.2) into a Neumann boundary value problem for which we recall standard estimates that will be needed for the arguments in the proofs of our stability results.

3.1. Technical results.

In what follows we recall standard estimates for the solution of Neumann boundary value problems of type

$$\begin{cases} \nabla \cdot (\sigma\nabla u) & = -\nabla \cdot E \quad \text{in} \quad \Omega, \\ (\sigma\nabla u + E) \cdot \nu & = 0 \qquad\quad \text{on} \quad \partial\Omega. \end{cases} \tag{3.1}$$

Such estimates are standard in the theory of elliptic partial differential equations and we recall them, together with their proof, for the sake of completeness. For a detailed proof, we recall [8, section 2], [37, section 2].

Proposition 3.1. *Let $\sigma \in C^{1,\beta}(\overline{\Omega})$ be a matrix-valued function satisfying the uniform ellipticity condition*

$$\Lambda^{-1}|\xi|^2 \leq \sigma(x)\xi \cdot \xi \leq \Lambda|\xi|^2 \quad \text{for a.e. } x \in \bar{\Omega} \quad \forall \xi \in \mathbb{R}^3, \tag{3.2}$$

and let $E \in L^2(\Omega)$ be a vector-valued function. The Neumann problem (3.1) has a unique solution $u \in H^1(\Omega)$ (up to an additive constant) that satisfies

$$||\nabla u||_{L^2(\Omega)} \leq \Lambda||E||_{L^2(\Omega)}. \tag{3.3}$$

Proof. As a straighforward consequence of

$$\int_\Omega \sigma\nabla u\cdot\nabla u\,dx = -\int_\Omega E\cdot\nabla u\,dx, \tag{3.4}$$

we obtain

$$\Lambda^{-1}||\nabla u||^2_{L^2(\Omega)} \le \Big|-\int_\Omega E\cdot\nabla u dx\Big| \le ||E||_{L^2(\Omega)}||\nabla u||_{L^2(\Omega)}, \tag{3.5}$$

which concludes the proof. ∎

Proposition 3.2. *Let γ_i satisfy (2.4), (2.5) for $i=1,2$.*

1. *If $A\in\mathcal{A}$ and $\sigma_i(x)=A(\gamma_i(x))$, $x\in\overline{\Omega}$ for $i=1,2$, then we have*

$$||E_{A(\gamma_i)}||_{C^{1,\beta}(\Omega)} \le C_1 \qquad \text{for } i=1,2, \tag{3.6}$$

$$||E_{A(\gamma_1)}-E_{A(\gamma_2)}||_{L^2(\Omega)} \le C_3||\gamma_1-\gamma_2||_{L^2(\Omega)}, \tag{3.7}$$

   where $E_{A(\gamma_i)}$ is the unique solution to (1.2), with $\sigma_i=A(\gamma_i)$ for $i=1,2$ and C_1, C_3 are positive constants depending only on Λ, r_0, L, K, $\mathcal{E}_1$, M, and $\mu(\Omega)$.
2. *Similarly, if and $A\in\mathcal{A}'$ and $\sigma_i(x)=A(x,\gamma_i(x))$, $x\in\overline{\Omega}$ for $i=1,2$, then we have*

$$||E_{A(\cdot,\gamma_i)}||_{C^{1,\beta}(\Omega)} \le C_2 \qquad \text{for } i=1,2, \tag{3.8}$$

$$||E_{A(\cdot,\gamma_1)}-E_{A(\cdot,\gamma_2)}||_{L^2(\Omega)} \le C_4||\gamma_1-\gamma_2||_{L^2(\Omega)}, \tag{3.9}$$

   where $E_{A(\cdot,\gamma_i)}$ is the unique solution to (1.2), with $\sigma_i=A(\cdot,\gamma_i)$ for $i=1,2$, with C_2, C_4 being positive constants depending only on Λ, r_0, L, K, $\mathcal{E}_1$, $\boldsymbol{M}$, and $\mu(\Omega)$.

Proof. As the proof follows the same line of [8, Proof of Proposition 2], we only highlight the main steps of case 1. and only point out where case 2. differs from it, as such modifications are minor. For case 1. we start by noticing that for $\tilde{E}=\frac{1}{2}(-y,x,0)$ we have that $\nabla\times(E_{A(\gamma_i)}-\tilde{E})=0$ for $i=1,2$ and $E_{A(\gamma_i)}=\tilde{E}+\nabla u_i$, where u_i solves the Neumann problem

$$\begin{cases} \nabla\cdot(A(\gamma_i)\nabla u_i) & = -\nabla\cdot(A(\gamma_i)\tilde{E}) \quad \text{in} \quad \Omega,\\ (A(\gamma_i)\nabla u_i + A(\gamma_i)\tilde{E})\cdot\nu & = 0 \qquad\qquad\quad \text{on} \quad \partial\Omega \end{cases} \tag{3.10}$$

for $i=1,2$. Thus, estimate (3.6) is a straightforward consequence of (2.5) and Proposition 2.3 (see also [22, chapter 9], [23]).

To prove (3.7), we start by simplifying our notation. We denote $E_{A(\gamma_i)}$, simply with E_i for $i=1$, 2. Noting that $\nabla\times E_1=\nabla\times E_2$, we write

$$\nabla v = E_1 - E_2, \tag{3.11}$$

where v is the unique solution to

$$\begin{cases} \nabla\cdot(A(\gamma_1)\nabla v) & = -\nabla\cdot((A(\gamma_1)-A(\gamma_2))E_2) \quad \text{in} \quad \Omega,\\ (A(\gamma_1)\nabla v + (A(\gamma_1)-A(\gamma_2))E_2)\cdot\nu & = 0 \qquad\qquad\quad \text{on} \quad \partial\Omega \end{cases} \tag{3.12}$$

and

$$\int_{\partial\Omega} v = 0. \tag{3.13}$$

Thus by Cauchy–Schwarz we obtain

$$\int_\Omega A(\gamma_1)\nabla v \cdot \nabla v dx \leq \int_\Omega ((A(\gamma_1) - A(\gamma_2))E_2) \cdot \nabla v \, dx, \tag{3.14}$$

which, combined with (3.6) and the uniform ellipticity condition (2.3), leads to

$$||\nabla v||_{L^2(\Omega)} \leq \Lambda C_1 ||A(\gamma_1) - A(\gamma_2)||_{L^2(\Omega)}. \tag{3.15}$$

From the Lagrange theorem, for every $x \in \Omega$, there exists $t(x)$, $0 < t(x) < 1$, such that

$$A(\gamma_1(x)) - A(\gamma_2(x)) = (\gamma_1 - \gamma_2)(x) \left.\frac{dA(t)}{dt}\right|_{t=c(x)}, \tag{3.16}$$

where $c(x) = \gamma_2(x) + t(x)(\gamma_1(x) - \gamma_2(x))$. Hence we obtain

$$||\nabla v||_{L^2(\Omega)} \leq \Lambda C_1 ||\gamma_1 - \gamma_2||_{L^2(\Omega)} \left|\left| \left.\frac{dA(t)}{dt}\right|_{t=c(\cdot)} \right|\right|_{L^\infty(\Omega)} \tag{3.17}$$

and

$$||E_1 - E_2||_{L^2(\Omega)} \leq C_3 ||\gamma_1 - \gamma_2||_{L^2(\Omega)}, \tag{3.18}$$

where $C_3 = \Lambda \mathcal{E}_1 C_1$.

For case 2., estimate (3.8) follows, similarly to (3.6), from (2.5) and Proposition 2.6. With a similar argument to case 1., from the Lagrange theorem, for every $x \in \Omega$, there exists $t(x)$, $0 < t(x) < 1$, such that

$$A(x, \gamma_1(x)) - A(x, \gamma_2(x)) = (\gamma_1 - \gamma_2)(x) \left.\frac{\partial A(x,\, t)}{\partial t}\right|_{t=c(x)}, \tag{3.19}$$

where $c(x) = \gamma_2(x) + t(x)(\gamma_1(x) - \gamma_2(x))$, which leads to

$$||E_1 - E_2||_{L^2(\Omega)} \leq \Lambda C_1 ||\gamma_1 - \gamma_2||_{L^2(\Omega)} \left|\left| \left.\frac{\partial A(\cdot,\, t)}{\partial t}\right|_{t=c(\cdot)} \right|\right|_{L^\infty(\Omega)}, \tag{3.20}$$

hence

$$||E_1 - E_2||_{L^2(\Omega)} \leq C_4 ||\gamma_1 - \gamma_2||_{L^2(\Omega)}, \tag{3.21}$$

where $C_4 = \Lambda \mathcal{E}_2 C_2$. ∎

3.2. Proof of the stability estimates.

Proof of Theorem 2.7. We write the difference in the data $F_1 - F_2$ as

$$\begin{aligned} F_1 - F_2 &= \nabla \cdot \Big(A(\gamma_1) E_1 \times B_0 \Big) - \nabla \cdot \Big(A(\gamma_2) E_2 \times B_0 \Big) \\ &= \nabla \cdot \Big((A(\gamma_1) - A(\gamma_2)) E_1 \times B_0 \Big) + \nabla \cdot \Big(A(\gamma_2)(E_1 - E_2) \times B_0 \Big), \end{aligned} \tag{3.22}$$

and from the Lagrange theorem, for every $x \in \Omega$, there exists $t(x)$, $0 < t(x) < 1$, such that

$$F_1 - F_2 = \nabla \cdot \left((\gamma_1 - \gamma_2) \frac{dA}{dt}(t)\Big|_{t=c(\cdot)} E_1 \times B_0 \right) + \nabla \cdot \Big(A(\gamma_2)\,(E_1 - E_2) \times B_0 \Big), \tag{3.23}$$

where $c(x) = \gamma_2(x) + t(x)(\gamma_1(x) - \gamma_2(x))$. Then, we can split $F_1 - F_2$ into three contributions

$$F_1 - F_2 = I_1 + I_2 + I_3, \tag{3.24}$$

where

$$\begin{aligned} I_1 &= \nabla \cdot \Big((\gamma_1 - \gamma_2) E_1 \times B_0 \Big), \\ I_2 &= \nabla \cdot \left((\gamma_1 - \gamma_2) \left(\frac{dA}{dt}(t)\Big|_{t=c(\cdot)} - I \right) E_1 \times B_0 \right), \\ I_3 &= \nabla \cdot \Big(A(\gamma_2)(E_1 - E_2) \times B_0 \Big), \end{aligned} \tag{3.25}$$

where I denotes the 3×3 identity matrix. To extract information about $\gamma_1 - \gamma_2$ in Ω we multiply the data difference $F_1 - F_2$ by $\gamma_1 - \gamma_2$ and integrate over Ω. We do this by considering each contribution I_i, $i = 1, 2, 3$, to the data separately. Starting with I_1, we obtain

$$\begin{aligned} \int_\Omega (\gamma_1 - \gamma_2) I_1 dx &= \int_\Omega (\gamma_1 - \gamma_2)^2 \nabla \cdot (E_1 \times B_0) \\ &\quad + \frac{1}{2} \nabla (\gamma_1 - \gamma_2)^2 \cdot (E_1 \times B_0) dx \\ &= \frac{1}{2} \int_\Omega (\gamma_1 - \gamma_2)^2 \nabla \cdot (E_1 \times B_0) dx \\ &= \frac{1}{2} ||\gamma_1 - \gamma_2||^2_{L^2(\Omega)}, \end{aligned} \tag{3.26}$$

where in the second equality of (3.26) we performed integration by parts and used the fact that γ_1 and γ_2 share the same boundary values. In the last equality, we used the fact that $\nabla \cdot (E_1 \times B_0) = 1$.

Multiplying I_2 by $\gamma_1 - \gamma_2$, we have

$$\begin{aligned} \left| \int_\Omega (\gamma_1 - \gamma_2) I_2 dx \right| &= \Big| \int_\Omega (\gamma_1 - \gamma_2)^2 \nabla \cdot \left(\left(\frac{dA}{dt}(t)\Big|_{t=c(\cdot)} - I \right) E_1 \times B_0 \right) \\ &\quad + (\gamma_1 - \gamma_2) \nabla (\gamma_1 - \gamma_2) \cdot \left(\left(\frac{dA}{dt}(t)\Big|_{t=c(\cdot)} - I \right) E_1 \times B_0 \right) dx \Big| \\ &= \left| \int_\Omega (\gamma_1 - \gamma_2) \nabla (\gamma_1 - \gamma_2) \cdot \left(\left(\frac{dA}{dt}(t)\Big|_{t=c(\cdot)} - I \right) E_1 \times B_0 \right) dx \right| \\ &\leq \mathcal{C} C_1 (\mathcal{E}_1 + 1) ||\gamma_1 - \gamma_2||^2_{L^2(\Omega)}, \end{aligned} \tag{3.27}$$

where in the second equality of (3.27) we again performed integration by parts and again recalled that γ_1 and γ_2 share the same boundary. In the inequality, estimate (2.2), (2.14), and (3.6) have been used.

Finally, multiplying I_3 by $\gamma_1 - \gamma_2$, leads to

$$\begin{aligned} \left|\int_\Omega (\gamma_1-\gamma_2) I_3 dx\right| &= \left|\int_\Omega \nabla(\gamma_1-\gamma_2)\cdot\Big(A(\gamma_2)(E_1-E_2)\times B_0\Big)dx\right| \\ &\le \mathcal{C}\Lambda C_3 ||\gamma_1-\gamma_2||^2_{L^2(\Omega)}, \end{aligned} \tag{3.28}$$

where the first equality in (3.28) is derived again by performing integration by parts and noticing that γ_1 and γ_2 share the same boundary values. In the inequality, (2.3), assumption (2.14), and (3.7) have been used.

Hence, for $\mathcal{C}C_1(\mathcal{E}_1+1)+\mathcal{C}\Lambda C_3 < \frac{1}{2}$, we obtain

$$\int_\Omega (\gamma_1-\gamma_2)(F_1-F_2)dx \ge C||\gamma_1-\gamma_2||^2_{L^2(\Omega)}, \tag{3.29}$$

where $C = \frac{1}{2} - \mathcal{C}\Big(C_1(\mathcal{E}_1+1)+\Lambda C_3\Big) > 0$, which concludes the proof. ∎

Proof of Theorem 2.8. Similarly to the proof of theorem 2.7, we write the data difference as

$$\begin{aligned} \tilde{F}(\gamma_1)-\tilde{F}(\gamma_2) &= \nabla\cdot(A(\cdot,\gamma_1)E_1\times B_0) - \nabla\cdot(A(\cdot,\gamma_2)E_2\times B_0) \\ &= \nabla\cdot((A(\cdot,\gamma_1)-A(\cdot,\gamma_2))E_1\times B_0) + \nabla\cdot(A(\cdot,\gamma_2)(E_1-E_2)\times B_0). \end{aligned} \tag{3.30}$$

From the Lagrange theorem, for every $x\in\Omega$, there exists $t(x)$, $0<t(x)<1$, such that

$$A(x,\gamma_1)-A(x,\gamma_2) = (\gamma_1-\gamma_2)(x)\frac{\partial A(x,t)}{\partial t}\Big|_{t=c(x)}, \tag{3.31}$$

where $c(x)=\gamma_2(x)+t(x)(\gamma_1(x)-\gamma_2(x))$. Therefore, we obtain

$$\tilde{F}_1-\tilde{F}_2 = \nabla\cdot\Big((\gamma_1-\gamma_2)\frac{\partial A(\cdot,t)}{\partial t}\Big|_{t=c(x)}E_1\times B_0\Big) + \nabla\cdot(A(\cdot,\gamma_2)(E_1-E_2)\times B_0). \tag{3.32}$$

By splitting again $\tilde{F}_1-\tilde{F}_2$ as

$$\tilde{F}_1-\tilde{F}_2 = I_1+I_2+I_3, \tag{3.33}$$

where

$$\begin{aligned} I_1 &= \nabla\cdot\Big((\gamma_1-\gamma_2)E_1\times B_0\Big), \\ I_2 &= \nabla\cdot\left((\gamma_1-\gamma_2)\left(\frac{\partial A(\cdot,t)}{\partial t}\Big|_{t=c(\cdot)} - I\right)E_1\times B_0\right), \\ I_3 &= \nabla\cdot\Big(A(\cdot,\gamma_2)(E_1-E_2)\times B_0\Big), \end{aligned} \tag{3.34}$$

with a similar procedure as that of the proof of Theorem 2.7 we obtain the following estimates:

$$\int_\Omega (\gamma_1-\gamma_2)I_1 dx = \frac{1}{2}||\gamma_1-\gamma_2||^2_{L^2(\Omega)}, \tag{3.35}$$

$$\left|\int_\Omega (\gamma_1-\gamma_2)I_2 dx\right| = \left|\int_\Omega (\gamma_1-\gamma_2)\nabla(\gamma_1-\gamma_2)\cdot\left(\left(\frac{\partial A(\cdot,t)}{\partial t}\Big|_{t=c(\cdot)} - I\right)E_1\times B_0\right)dx\right| \tag{3.36}$$
$$\leq \mathcal{C}C_2(\mathcal{E}_2+1)||\gamma_1-\gamma_2||^2_{L^2(\Omega)},$$

$$\left|\int_\Omega (\gamma_1-\gamma_2)I_3 dx\right| = \left|\int_\Omega \nabla(\gamma_1-\gamma_2)\cdot(A(\cdot,\gamma_2(\cdot))\,(E_1-E_2)\times B_0)dx\right| \tag{3.37}$$
$$\leq \mathcal{C}\Lambda C_4||\gamma_1-\gamma_2||^2_{L^2(\Omega)}.$$

By combining (3.35)–(3.37) together and choosing the parameters such that $(\mathcal{C}C_2(\mathcal{E}_2+1)+\mathcal{C}\Lambda C_4)<\frac{1}{2}$, we finally obtain

$$\int_\Omega (\gamma_1-\gamma_2)(\tilde{F}(\gamma_1)-\tilde{F}(\gamma_2))dx \geq \tilde{C}||\gamma_1-\gamma_2||^2_{L^2(\Omega)}, \tag{3.38}$$

where $\tilde{C}=\frac{1}{2}-(\mathcal{C}C_2(\mathcal{E}_2+1)+\mathcal{C}\Lambda C_4)>0$, which concludes the proof. ∎

4. Reconstruction of γ.

4.1. The functional framework and the algorithm. We denote by γ_* the true scalar function to be reconstructed, leading to the true anisotropic conductivities $A_* := A(\gamma_*)$ and $A_* := A(\cdot,\gamma_*)$, when $A\in\mathcal{A}$ and $A\in\mathcal{A}'$, respectively. When $A\in\mathcal{A}$, the forward operator is

$$F(\gamma) = \nabla\cdot(A(\gamma)E_{A(\gamma)}\times B_0), \tag{4.1}$$

where $E_A := E_{A(\gamma)}$ solves

$$\begin{cases} \nabla\times E_A = B_0 & \text{in } \Omega,\\ \nabla\cdot A(\gamma)E_A = 0 & \text{on } \Omega,\\ A(\gamma)E_A\cdot\nu = 0 & \text{on } \partial\Omega, \end{cases} \tag{4.2}$$

and the scalar function γ is updated by solving a stationary advection-diffusion equation as shown in Algorithm 4.1 below. Similarly, when $A\in\mathcal{A}'$, the forward operator is

$$\tilde{F}(\gamma) = \nabla\cdot(A(\cdot,\gamma)E_A\times B_0), \tag{4.3}$$

where $E_A := E_{A(\cdot,\gamma)}$ solves

$$\begin{cases} \nabla\times E_A = B_0 & \text{in } \Omega,\\ \nabla\cdot A(\cdot,\gamma)E_A = 0 & \text{on } \Omega,\\ A(\cdot,\gamma)E_A\cdot\nu = 0 & \text{on } \partial\Omega, \end{cases} \tag{4.4}$$

and the scalar function γ together with the electric field E are updated as per Algorithm 4.1.

4.2. Convergence analysis. Under a smallness condition on $\frac{dA(t)}{dt}$ and $\frac{\partial A(\cdot,t)}{dt}$, on $[\lambda^{-1},\lambda]$ with respect to I, for $A\in\mathcal{A}$ and $A\in\mathcal{A}'$, respectively (see (4.9) and (4.13), respectively), we obtain the following convergence results.

Algorithm 4.1 (reconstruction)

- We choose an initial conductivity γ_1 satisfying (2.4), (2.5) and set $k=1$.
- At step k, defining $A_k := A(\gamma_k)$, we solve the boundary value problem

$$\left\{\begin{array}{lll} \nabla \times E_k &= B_0 & \text{in} \quad \Omega, \\ \nabla \cdot A_k E_k &= 0 & \text{on} \quad \Omega, \\ A_k E_k \cdot \nu &= 0 & \text{on} \quad \partial\Omega \end{array}\right. \tag{4.5}$$

to update the electric field E_k.

- By solving the stationary advection-diffusion equation with the inflow boundary condition, we calculate the updated conductivity $A_{k+1/2} := A(\gamma_{k+1})$ as follows:

$$\left\{\begin{array}{lll} \nabla \cdot (A_{k+1/2} E_k \times B_0) &= \nabla \cdot (A_* E_{A_*} \times B_0) & \text{in} \quad \Omega, \\ \gamma_{k+1} &= \gamma_* & \text{on} \quad \partial\Omega^-, \end{array}\right. \tag{4.6}$$

where

$$\partial\Omega^- = \left\{ x \in \partial\Omega \;\middle|\; \frac{dA(t)}{dt}\Big|_{t=\gamma_*(x)} E_k(x) \times B_0 \cdot \nu(x) < 0 \right\} \quad \text{for} \quad A \in \mathcal{A},$$

and

$$\partial\Omega^- = \left\{ x \in \partial\Omega \;\middle|\; \frac{\partial A(x,t)}{\partial t}\Big|_{t=\gamma_*(x)} E_k(x) \times B_0 \cdot \nu(x) < 0 \right\} \quad \text{for} \quad A \in \mathcal{A}'.$$

Theorem 4.1. *Suppose that the true scalar function γ_* satisfies (2.4), (2.5) and that the true conductivity $A_* = A(\gamma_*)$ satisfies*

$$\nabla \cdot (A_* \xi \times B_0) \le \widetilde{\mathcal{F}}_1 \nabla \cdot (\gamma_* \xi \times B_0) \quad \textit{for any} \quad x \in \mathbb{R}^3, \quad \textit{for any} \quad \xi \in \mathbb{R}^3 \tag{4.7}$$

for some constant $\widetilde{\mathcal{F}}_1 > 0$. Let $A \in \mathcal{A}$ and, additionally, assume that

$$\frac{dA}{dt} \in C^1\left([\lambda^{-1}, \lambda], Sym\right) \tag{4.8}$$

and that there is a constant $\tilde{\mathcal{E}}_1$, $0 < \tilde{\mathcal{E}}_1 < 1$ such that

$$\sup_{t\in[\lambda^{-1},\lambda]} \sup_{x\in\Omega} \left| \nabla \cdot \left[\left(\frac{dA}{dt} - I \right) E_k \times B_0 \right] \right| \le \tilde{\mathcal{E}}_1. \tag{4.9}$$

If either

1.

$$\gamma_k = \gamma_* \qquad \textit{on} \quad \partial\Omega, \quad \textit{for any} \quad k, \quad k \ge 1;$$

or

2.

$$\gamma_k = \gamma_* \quad \text{on} \quad \partial\Omega^- \quad \text{and} \quad \sup_{t\in[\lambda^{-1},\lambda]} \frac{dA}{dt} E_k \times B_0 \cdot \nu \geq 0 \quad \text{on} \quad \partial\Omega^+,$$
$$\text{for any} \quad k, \quad k \geq 1,$$

then, for an appropriate choice of $\mathcal{C}$, Λ, C_1, $\tilde{C}_3$, $\mathcal{E}_1$, *and* $\tilde{\mathcal{E}}_1$, *there exists a constant* C, $0 < C < 1$ *such that*

$$||\gamma_{k+1} - \gamma_*||_{L^2(\Omega)} \leq C||\gamma_k - \gamma_*||_{L^2(\Omega)}. \tag{4.10}$$

Theorem 4.2. *Suppose that the true scalar function* γ_* *satisfies the conditions of Theorem 4.1 above and that the true conductivity* $A_* = A(\cdot, \gamma_*)$ *satisfies*

$$\nabla \cdot (A_* \xi \times B_0) \leq \widetilde{\mathcal{F}}_2 \nabla \cdot (\gamma_* \xi \times B_0) \quad \text{for any} \quad x \in \mathbb{R}^3, \quad \text{for any} \quad \xi \in \mathbb{R}^3 \tag{4.11}$$

for some constant $\widetilde{\mathcal{F}}_2 > 0$. *Let* $A \in \mathcal{A}'$, *and, additionally, assume that*

$$\frac{\partial A(\cdot, t)}{\partial t} \in C^1(\overline{\Omega} \times [\lambda^{-1}, \lambda], Sym) \tag{4.12}$$

and there exists a constant $\tilde{\mathcal{E}}_2$, $0 < \tilde{\mathcal{E}}_2 < 1$ *such that*

$$\sup_{t\in[\lambda^{-1},\lambda]} \sup_{x\in\Omega} \left| \nabla \cdot \left[\left(\frac{\partial A}{\partial t}(\cdot, t)\Big|_{t=c(\cdot)} - I \right) E_k \times B_0 \right] \right| \leq \tilde{\mathcal{E}}_2. \tag{4.13}$$

If either

1.

$$\gamma_k = \gamma_* \quad \text{on} \quad \partial\Omega \quad \text{for any} \quad k, \quad k \geq 1;$$

or

2.

$$\gamma_k = \gamma_* \quad \text{on} \quad \partial\Omega^- \quad \text{and} \quad \sup_{t\in[\lambda^{-1},\lambda]} \frac{\partial A(\cdot, t)}{\partial t} E_k \times B_0 \cdot \nu \geq 0 \quad \text{on} \quad \partial\Omega^+$$
$$\text{for any} \quad k, \quad k \geq 1.$$

Then, for an appropriate choice of $\mathcal{C}$, Λ, C_2, $\tilde{C}_4$ $\mathcal{E}_2$, *and* $\tilde{\mathcal{E}}_2$, *there exists a constant* C $0 < C < 1$ *such that*

$$||\gamma_{k+1} - \gamma_*||_{L^2(\Omega)} \leq C||\gamma_k - \gamma_*||_{L^2(\Omega)}. \tag{4.14}$$

Proof of Theorem 4.1. We start by subtracting $\nabla \cdot (A_* E_k \times B_0)$ from both sides of the first equation in (4.6), which leads to

$$\nabla \cdot ((A_{k+1} - A_*) E_k \times B_0) = \nabla \cdot (A_*(E_* - E_k) \times B_0). \tag{4.15}$$

Multiplying by $\gamma_{k+1}-\gamma_*$ and integrating over Ω yields

$$\int_\Omega(\gamma_{k+1}-\gamma_*)\nabla\cdot((A_{k+1}-A_*)E_k\times B_0)=\int_\Omega(\gamma_{k+1}-\gamma_*)\nabla\cdot(A_*(E_*-E_k)\times B_0). \tag{4.16}$$

Using the property that

$$A\in C^1\left([\lambda^{-1},\lambda],Sym\right) \tag{4.17}$$

from the Lagrange theorem, for every $x\in\Omega$, there exists $t(x)$, $0<t(x)<1$, such that

$$A_{k+1}-A(\gamma_*)=(\gamma_{k+1}-\gamma_*)\frac{dA}{dt}(t)\Big|_{t=c(x)}, \tag{4.18}$$

where $c(x)=\gamma_{k+1}(x)+t(x)(\gamma_*(x)-\gamma_{k+1}(x))$, hence we get

$$\int_\Omega(\gamma_{k+1}-\gamma_*)\nabla\cdot\Big((\gamma_{k+1}-\gamma_*)\frac{dA}{dt}(t)\Big|_{t=c(\cdot)}E_k\times B_0\Big)=\int_\Omega(\gamma_{k+1}-\gamma_*)\nabla\cdot(A_*(E_*-E_k)\times B_0). \tag{4.19}$$

The term on the left-hand side of (4.19) can be estimated from below as follows:

$$\begin{aligned}
&\int_\Omega(\gamma_{k+1}-\gamma_*)\nabla\cdot\Big((\gamma_{k+1}-\gamma_*)\frac{dA}{dt}(t)\Big|_{t=c(\cdot)}E_k\times B_0\Big)dx\\
=&\frac{1}{2}\int_{\partial\Omega}(\gamma_{k+1}-\gamma_*)^2\cdot\left(\frac{dA}{dt}(t)\Big|_{t=c(\cdot)}E_k\times B_0\right)\cdot\nu ds(x)\\
&+\frac{1}{2}\int_\Omega(\gamma_{k+1}-\gamma_*)^2\nabla\cdot\left(\frac{dA}{dt}(t)\Big|_{t=c(\cdot)}E_k\times B_0\right)dx,\\
\geq&\frac{1}{2}\int_{\partial\Omega}(\gamma_{k+1}-\gamma_*)^2\cdot\left(\frac{dA}{dt}(t)\Big|_{t=c(\cdot)}E_k\times B_0\right)\cdot\nu ds(x)\\
&+\frac{1}{2}||(\gamma_{k+1}-\gamma_*)||^2_{L^2(\Omega)}\\
&-\frac{1}{2}\int_\Omega|\gamma_{k+1}-\gamma_*|^2\quad\sup_\Omega\left|\nabla\cdot\left(\left(\frac{dA}{dt}(t)\Big|_{t=c(\cdot)}-I\right)E_k\times B_0\right)\right|dx.
\end{aligned} \tag{4.20}$$

In the second equality in (4.20) we performed integration by parts twice. In either cases 1. or 2., (4.20), combined with (4.9), leads to

$$\begin{aligned}
&\int_\Omega(\gamma_{k+1}-\gamma_*)\nabla\cdot\Big((\gamma_{k+1}-\gamma_*)\frac{dA}{dt}(t)\Big|_{t=c(\cdot)}E_k\times B_0\Big)dx\\
&\geq\frac{1}{2}(1-\tilde{\mathcal{E}}_1)||(\gamma_{k+1}-\gamma_*)||^2_{L^2(\Omega)}.
\end{aligned} \tag{4.21}$$

The term on the right hand side of (4.19) can be estimated from above as

$$\begin{aligned}
&\left|\int_\Omega(\gamma_{k+1}-\gamma_*)\nabla\cdot(A_*(E_*-E_k)\times B_0)\right|\\
&\leq||\gamma_{k+1}-\gamma_*||_{L^2(\Omega)}\,||\nabla\gamma_*||_{L^\infty(\Omega)}\,||(E_*-E_k)||_{L^2(\Omega)},\\
&\leq KC_3\widetilde{\mathcal{F}}_1|||\gamma_{k+1}-\gamma_*||_{L^2(\Omega)}||\gamma_*-\gamma_k||_{L^2(\Omega)},
\end{aligned} \tag{4.22}$$

where we combined estimates (4.7), together with (2.5) and (3.7). Choosing $\frac{KC_3\tilde{\mathcal{F}}_1}{1-\tilde{\mathcal{E}}_1} \leq \frac{1}{2}$, we finally derive

$$||\gamma_{k+1}-\gamma_*||_{L^2(\Omega)} \leq C||\gamma_k-\gamma_*||_{L^2(\Omega)}, \tag{4.23}$$

where $0<C<1$. ∎

Proof of Theorem 4.2. As this proof is very similar to the one above, we only point where the two proofs slightly differ. In particular, we take care to point out what are the a priori constants that come into play. As above, subtracting $\nabla\cdot(A_*E_k\times B_0)$ from both sides of the first equation in (4.6) leads to

$$\nabla\cdot((A_{k+1}-A_*)E_k\times B_0)=\nabla\cdot(A_*(E_*-E_k)\times B_0). \tag{4.24}$$

Multiplying by $\gamma_{k+1}-\gamma_*$ and integrating over Ω yields

$$\int_\Omega(\gamma_{k+1}-\gamma_*)\nabla\cdot((A_{k+1}-A_*)E_k\times B_0)=\int_\Omega(\gamma_{k+1}-\gamma_*)\nabla\cdot(A_*(E_*-E_k)\times B_0). \tag{4.25}$$

Using the property that

$$A\in C^1\left(\overline{\Omega}\times[\lambda^{-1},\lambda],Sym\right) \tag{4.26}$$

from the Lagrange theorem, for every $x\in\Omega$, there exists $t(x)$, $0<t(x)<1$, such that

$$A(x,\gamma_{k+1})-A(x,\gamma_*)=(\gamma_{k+1}-\gamma_*)(x)\frac{\partial A(x,t)}{\partial t}\Big|_{t=c(x)}, \tag{4.27}$$

where $c(x)=\gamma_{k+1}(x)+t(x)(\gamma_*(x)-\gamma_{k+1}(x))$, hence we have

$$\int_\Omega(\gamma_{k+1}-\gamma_*)\nabla\cdot\left((\gamma_{k+1}-\gamma_*)\frac{\partial A(\cdot,t)}{\partial t}\Big|_{t=c(\cdot)}E_k\times B_0\right)=\int_\Omega(\gamma_{k+1}-\gamma_*)\nabla\cdot(A_*(E_*-E_k)\times B_0). \tag{4.28}$$

Arguing as above, the left-hand side of (4.28) can be estimated from below as

$$\begin{aligned}&\int_\Omega(\gamma_{k+1}-\gamma_*)\nabla\cdot\left((\gamma_{k+1}-\gamma_*)\frac{\partial A(\cdot,t)}{\partial t}\Big|_{t=c(\cdot)}E_k\times B_0\right)dx\\&\geq\frac{1}{2}\int_{\partial\Omega}(\gamma_{k+1}-\gamma_*)^2\cdot\left(\frac{\partial A(\cdot,t)}{\partial t}\Big|_{t=c(\cdot)}E_k\times B_0\right)\cdot\nu ds(x)\\&\quad+\frac{1}{2}||(\gamma_{k+1}-\gamma_*)||^2_{L^2(\Omega)}\\&\quad-\frac{1}{2}\int_\Omega|\gamma_{k+1}-\gamma_*|^2\quad\sup_\Omega\left|\nabla\cdot\left(\left(\frac{\partial A(\cdot,t)}{\partial t}\Big|_{t=c(\cdot)}-I\right)E_k\times B_0\right)\right|dx.\end{aligned} \tag{4.29}$$

and again, in either case, 1. or 2., (4.29), combined together with (4.13), leads to

$$\begin{aligned}&\int_\Omega(\gamma_{k+1}-\gamma_*)\nabla\cdot\left((\gamma_{k+1}-\gamma_*)\frac{\partial A(\cdot,t)}{\partial t}\Big|_{t=c(\cdot)}E_k\times B_0\right)dx\\&\geq\frac{1}{2}(1-\tilde{\mathcal{E}}_2)||(\gamma_{k+1}-\gamma_*)||^2_{L^2(\Omega)}.\end{aligned} \tag{4.30}$$

The right-hand side of (4.28) can be estimated from above as

$$\begin{aligned} &\left| \int_\Omega (\gamma_{k+1} - \gamma_*) \nabla \cdot (A_*(E_* - E_k) \times B_0) \right| \\ &\leq K C_4 \widetilde{F}_2 ||\gamma_{k+1} - \gamma_*||_{L^2(\Omega)} ||\gamma_* - \gamma_k||_{L^2(\Omega)}, \end{aligned} \tag{4.31}$$

where we combined estimates (4.11), together with (2.5) and (3.9). Therefore, choosing $\frac{KC_4\widetilde{F}_2}{1-\tilde{\mathcal{E}}_2} \leq \frac{1}{2}$, we derive

$$||\gamma_{k+1} - \gamma_*||_{L^2(\Omega)} \leq C ||\gamma_k - \gamma_*||_{L^2(\Omega)}. \tag{4.32}$$

■

5. Numerical experiments. In this section we present several numerical experiments where we implement the algorithm described in section 4. In each case, a scalar reference medium $\gamma_* \in \tilde{S}$ (the true scalar function to be reconstructed) is chosen, along with a specific choice of a 3×3 matrix function A belonging to either $\mathcal{A}$ or $\mathcal{A}'$. We start by considering a number of examples in which $A \in \mathcal{A}$ only (Examples 1–4). We consider the more general case of $A \in \mathcal{A}'$ in Examples 5 and 7, and in Example 6 we add noise to the source data to test the algorithm's resistance to noise.

We then compute the synthetic acoustic source data

$$F(\gamma_*) = \nabla \cdot (A_{\gamma_*} E_* \times B_0), \tag{5.1}$$

where E_* is the electric field solution to (4.5) corresponding to γ_*. For simplicity, in our examples we always choose reference conductivity $\gamma_0 = 1$. We note that in our examples, we found that the extra hypotheses for the convergence proof were not needed in practice. In fact, in three of the examples below, γ_* is not in C^1 (Examples 4, 6, and 7, where γ_* is piecewise affine and piecewise constant). This is to test the reconstruction from nonsmooth data. Again, it will be part of future work to extend our theoretical framework of sections 2–4 to conductivities with lower regularity assumptions and a more general anisotropic structure.

To compute solutions to both (4.5) and (4.6), we use the Python suite FEniCS. As described in the proof of Proposition 3.2, we replace (4.5) with the Neumann problem (3.10) and solve numerically for $u_{k+1} = u$ using a standard variational formulation and piecewise linear finite elements. Recall then that E_{k+1} is given by

$$E_{k+1} = \nabla u_{k+1} + \tilde{E},$$

where $\tilde{E} = 0.5[-y, x, 0]^T$. We note that while (3.10) is always a linear conductivity equation, (4.6) changes more drastically for different choices of A. To compute solutions to this generally nonlinear transport equation, we used two different approaches; a discontinuous Galekin method and a built-in FEniCS nonlinear solver. We give more details about these in the first two examples.

Example 1. For our first example we choose A to be

$$A(\gamma) = \begin{bmatrix} \gamma & 0 & 0 \\ 0 & \gamma & 0 \\ 0 & 0 & 1 \end{bmatrix} \tag{5.2}$$

and reference medium γ_* to be the Gaussian curve independent of z:

$$\gamma_* = \exp\left(-\frac{(x-0.5)^2}{0.02} - \frac{(y-0.5)^2}{0.02}\right) + 1.$$

In this case the transport equation (4.6) for γ_{k+1} becomes

$$\begin{cases} \nabla \cdot (\gamma_{k+1}(E_k \times B_0)) = \nabla \cdot (\gamma_*(E_* \times B_0)) & \text{in } \Omega, \\ \gamma_{k+1} = \gamma_* & \text{on } \partial\Omega^-, \end{cases}$$

which is two-dimensional (2D) linear isotropic, as was studied previously in [8]. To solve this linear transport equation, we use a discontinuous Galerkin (DG) method with upwinding, which we now describe briefly. Given a mesh T_h of Ω, we let V be a finite-dimensional space containing functions not necessarily continuous across mesh elements. We define the "*upwinding*" term on the boundary of a triangle by

$$\bar{E}_k = 0.5((E_k \times B_0) \cdot \vec{n} + |(E_k \times B_0) \cdot \vec{n}|)$$

and denote the jump of a function on an internal edge E by

$$[[f]] = f^+ - f^-,$$

where f^+ (f^-) is its restriction to the edge from the outflow (inflow) direction, respectively. Then the variational formulation for the numerical transport problem is as follows:

find $\gamma_{k+1} = \gamma \in V$ such that, for all $v \in V$,

$$\int_{\partial\Omega} v\gamma(E_k \times B_0) \cdot \vec{n}\, ds + \sum_E \int_E [[v]][[\gamma \bar{E}_k]]\, dS - \int_\Omega \nabla v \cdot \gamma(E_k \times B_0)\, dx = \int_\Omega F(\gamma^*) v\, dx,$$

where $F(\gamma^*)$ is the source data (5.1). Note that the upwinding term provides numerical stability. We refer to [14] for more details on DG methods and upwinding. Figure 1 shows the true γ_*, plotted alongside its numerical reconstruction using the above algorithm.

Example 2. In this next example we add nonlinearity in the dependence of A on γ. To solve the transport equation (4.6) in this and all of the examples that follow, instead of DG, we use the Fenics nonlinear solver with higher order Lagrange elements. We choose here

$$A(\gamma) = \begin{bmatrix} 0.4(\gamma+1)^2 & 0.01 & 0 \\ 0.01 & 3\gamma & 0 \\ 0 & 0 & \gamma \end{bmatrix} \tag{5.3}$$

and reference conductivity γ_* to be a sum of Gaussian curves given by

$$\gamma_* = \exp\left(-\frac{(x-0.65)^2}{0.02} - \frac{(y-0.65)^2}{0.02}\right) + 0.5 * \exp\left(-\frac{(x-0.25)^2}{0.05} - \frac{(y-0.25)^2}{0.05}\right).$$

With the definitions above, the transport problem (4.6) becomes the nonlinear equation for $\gamma = \gamma_{k+1}$:

$$a_1\gamma^2 + a_2\gamma + a_3\gamma\gamma_x + a_4\gamma_x - a_5\gamma_y + c = F(\gamma_*) \qquad \text{in} \quad \Omega, \tag{5.4}$$

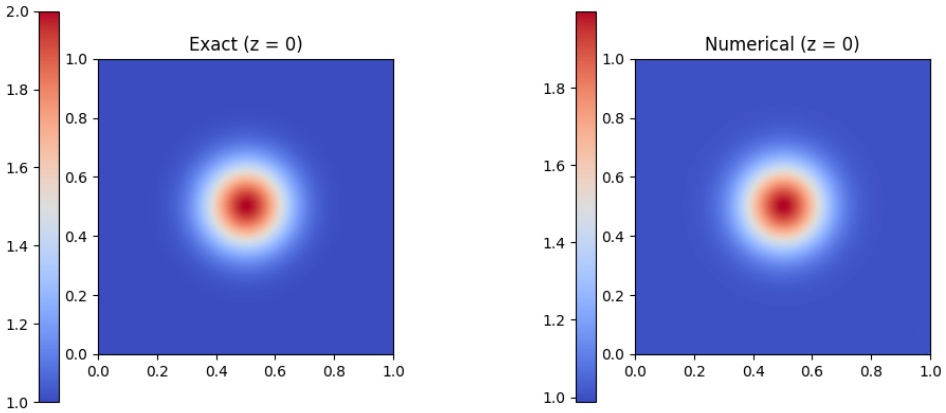

(a) *Reference conductivity* γ_* *at* $z = 0$ (b) *Reconstructed conductivity at* $z = 0$

Figure 1. *A given by* (5.2). *The resulting transport equation is linear. Ran for* 10 *iterations on a mesh of size* $150 \times 150 \times 1$.

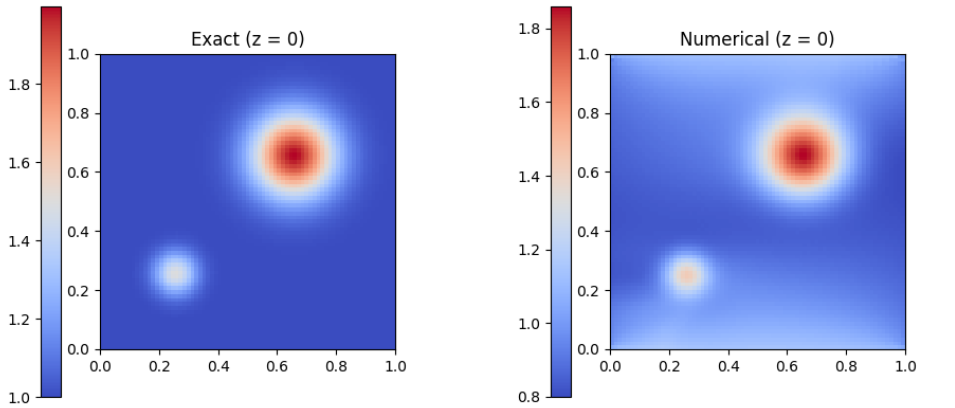

(a) *Reference conductivity* γ_* *at* $z = 0$ (b) *Reconstructed conductivity at* $z = 0$

Figure 2. *A given by* (5.3), *resulting in transport equation* (5.4). *Ran for* 10 *iterations on a mesh of size* $75 \times 75 \times 10$.

with inflow condition $\gamma = \gamma_*$ on $\partial\Omega^-$, where the spatially varying coefficients are functions of $E = [E_1, E_2, E_3]^T$, given by $a_1 = 0.4E_{2,x}$, $a_2 = 0.8E_{2,x} - 3E_{1,y}$, $a_3 = a_4 = 0.8E_2$, $a_5 = 3E_1$, and $c = 0.4E_{2,x}$. We show the reconstruction in Figure 2.

Example 3. In this next example we add nonlinearity on the off diagonals. Let

$$A(\gamma) = \begin{bmatrix} 0.4(\gamma+1)^2 & 0.01\gamma(1-\gamma) & 0 \\ 0.01\gamma(1-\gamma) & 3\gamma & 0 \\ 0 & 0 & \gamma \end{bmatrix}, \tag{5.5}$$

and let γ_* be given by

$$\gamma_*(x,y) = \cos\left(75(x-0.5)^2 + 75(y-0.5)^2\right) \exp\left(-\frac{(x-0.5)^2}{2} - \frac{(y-0.5)^2}{2}\right) + 1.$$

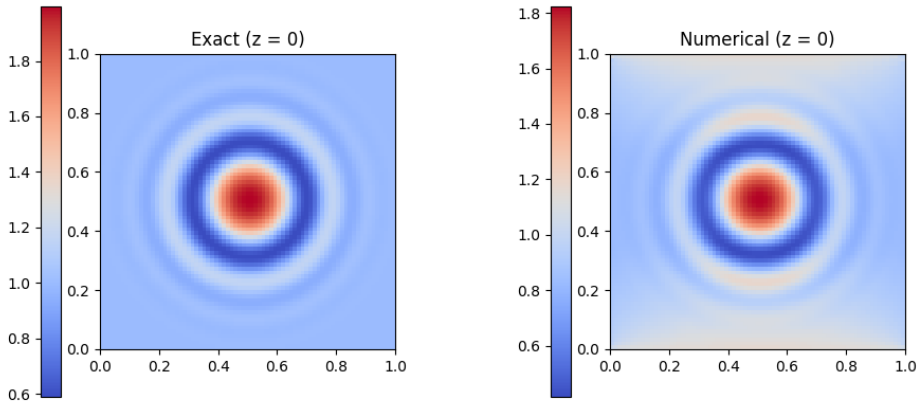

(a) *Reference conductivity* γ_* *at* $z = 0$ (b) *Reconstructed conductivity at* $z = 0$

Figure 3. *A given by* (5.5)*, yielding transport equation* (5.6)*. Ran for* 10 *iterations on a mesh of size* $75 \times 75 \times 10$.

In this case the transport equation (4.6) for $\gamma_{k+1} = \gamma$ becomes

$$a_1\gamma^2 + a_2\gamma\gamma_y + a_3\gamma_y + a_4\gamma + a_5\gamma_x + a_6\gamma\gamma_x + c = F(\gamma_*) \qquad \text{in} \quad \Omega, \tag{5.6}$$

with $\gamma = \gamma_*$ on $\partial\Omega^-$, where the coefficients are given by $a_1 = 0.4E_{2,x} + 0.01E_{1,x} - 0.01E_{2,y}$, $a_2 = 0.898E_2$, $a_3 = 0.01E_2 - 3E_1$, $a_4 = 0.8E_{2,x} - 0.01E_{1,x} + 0.01E_{2,y} - 3E_{1,y}$, $a_5 = 0.8E_2 - 0.01E_1$, $a_6 = 0.02E_1$, and $c = 0.4E_{2,x}$. Reconstruction results are in Figure 3.

Example 4. Here we choose a piecewise affine γ_* to test the reconstruction of nonsmooth conductivity. Let

$$A(\gamma) = \begin{bmatrix} 0.4(\gamma+1)^2 & \frac{1}{\gamma+20} & 0 \\ \frac{1}{\gamma+20} & 3\gamma & 0 \\ 0 & 0 & \gamma \end{bmatrix} \tag{5.7}$$

and define γ_* by

$$\gamma_*(x,y) = \begin{cases} 1 + 5(x - 0.3), & 0.3 \le x \le 0.5, \\ 2 - 5(x - 0.5), & 0.5 \le x \le 0.7, \\ 1 & \text{else.} \end{cases}$$

With the definitions above, the transport problem (4.6) becomes find $\gamma = \gamma_{k+1}$ such that

$$\begin{aligned} (E_{2,x} - E_{1,y})\gamma + (E_2)\gamma_x - \left(\frac{E_2}{(\gamma+20)^2} + E_1\right)\gamma_y \\ + \left(\frac{1}{\gamma+20}\right)\left(E_{2,y} - E_{1,x} + \frac{E_{1,x}}{\gamma+20}\right) = F(\gamma^*) \qquad \text{in} \quad \Omega, \end{aligned} \tag{5.8}$$

with $\gamma = \gamma_*$ on $\partial\Omega^-$. Numerical reconstructions are show in Figure 4.

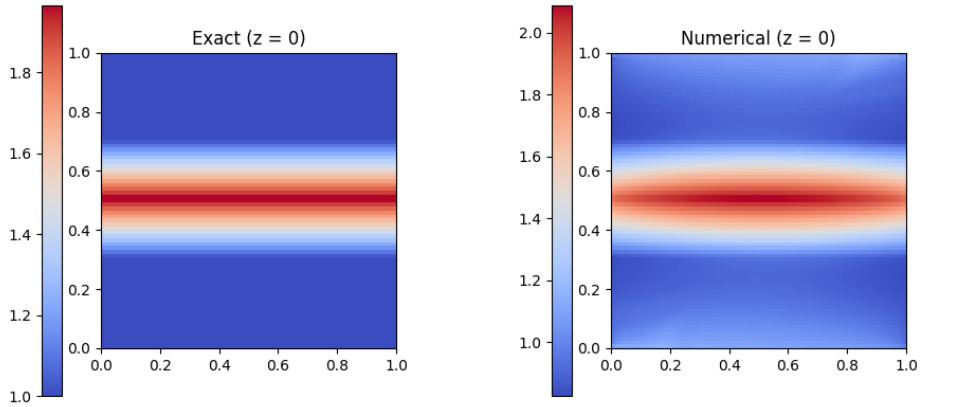

(a) *Reference conductivity* γ_* *at* $z = 0$ (b) *Reconstructed conductivity at* $z = 0$

Figure 4. *A given by* (5.7). *Ran for* 10 *iterations on a mesh of size* $75 \times 75 \times 10$.

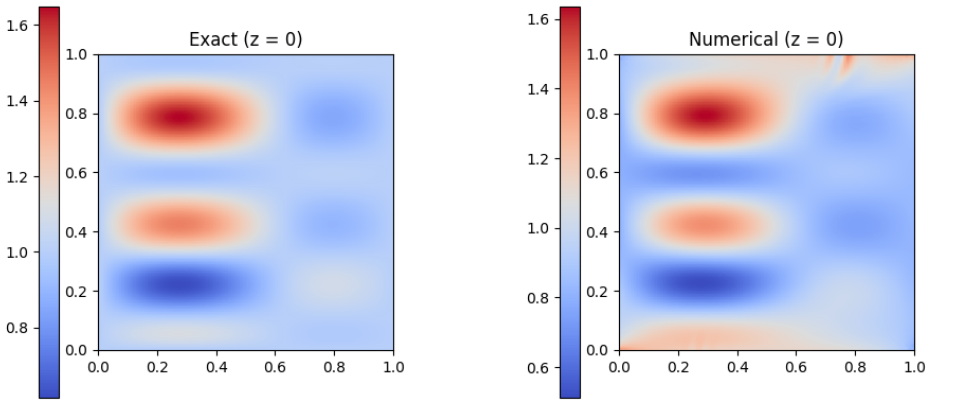

(a) *Reference conductivity* γ_* *at* $z = 0$ (b) *Reconstructed conductivity at* $z = 0$

Figure 5. *A given by* (5.9). *Ran for* 10 *iterations on a mesh of size* $100 \times 100 \times 10$.

Example 5. Next we choose A to be spatially varying as well as dependent on γ, as follows:

$$A(\vec{x}, \gamma) = \begin{bmatrix} 0.4(\gamma+1)^2 & 0.25(x^2+y^2)\gamma & 0 \\ 0.25(x^2+y^2)\gamma & 3\gamma & 0 \\ 0 & 0 & \gamma \end{bmatrix}, \tag{5.9}$$

and we let γ_* be the trigonometric function

$$\gamma_*(x, y) = \sin(10x)\sin(5y)\sin(7(1-x))\sin(y-1) + 1.$$

Numerical results are given in Figure 5.

Example 6. Next, we test the model's sensitivity to noisy data by adding random variable η to the source

$$F(\gamma_*) = \nabla \cdot (A_{\gamma_*} E_* \times B_0) + \eta, \tag{5.10}$$

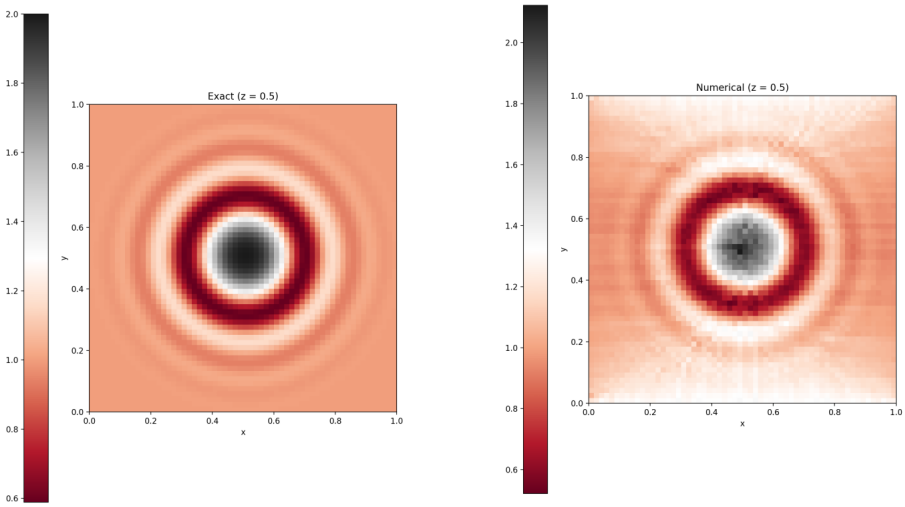

(a) *Reference conductivity* γ_* *at* $z = 0.5$ (b) *Reconstructed conductivity at* $z = 0.5$

Figure 6. *A given by* (5.9) *with noisy acoustic source data. Ran for* 20 *iterations on a mesh of size* $60 \times 60 \times 10$.

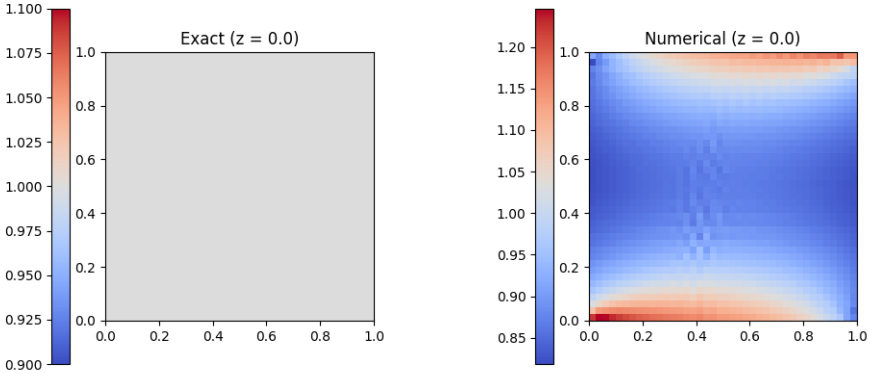

Figure 7. *Reconstruction for* (5.12) *at* $z = 0$.

where η is uniformly distributed averaging 9% of the maximum of the source data. We let

$$A(\gamma) = \begin{bmatrix} 0.4(\gamma+1)^2 & 0.01 & 0 \\ 0.01 & 3\gamma & 0 \\ 0 & 0 & \gamma \end{bmatrix}, \tag{5.11}$$

and we let γ_* be as in Example 3. The results are presented in Figure 6., where we can see that the reconstruction is quite stable in the presence of noise.

Example 7. Finally, we present an example in which A is spatially varying, as well as dependent on γ, and γ_* is z-dependent. We let

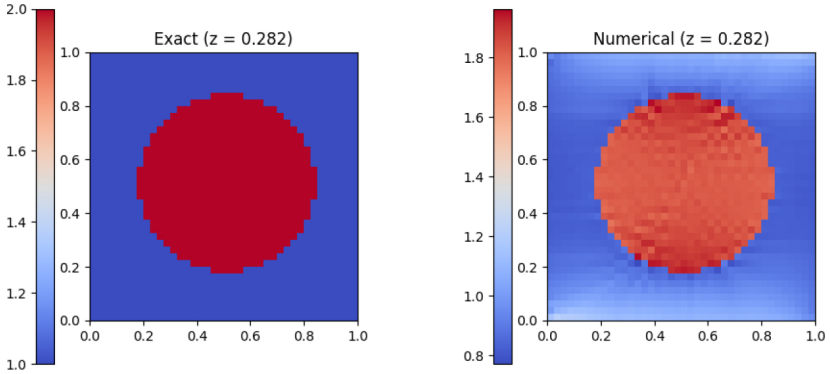

Figure 8. *Reconstruction for* (5.12) *at* $z = 0.282$.

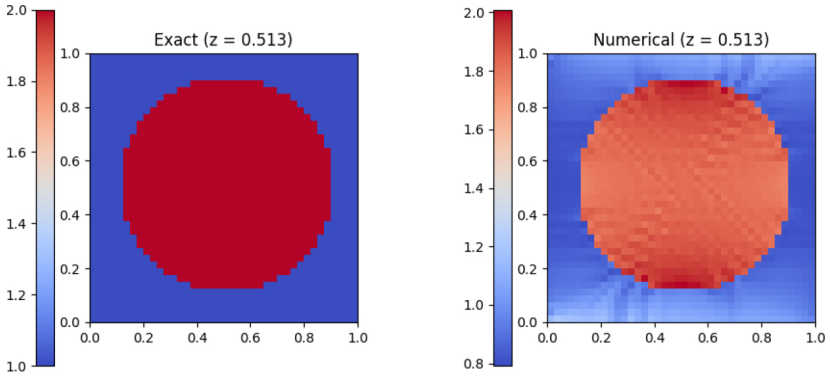

Figure 9. *Reconstruction for* (5.12) *at* $z = 0.513$.

$$A(\vec{x},\gamma) = \begin{bmatrix} 0.4(\gamma+1)^2 & 0.25((x-0.5)^2+(y-0.5)^2)\gamma & 0 \\ 0.25((x-0.5)^2+(y-0.5)^2)\gamma & 3\gamma & 0 \\ 0 & 0 & \gamma \end{bmatrix}, \tag{5.12}$$

and we let γ_* be a piecewise constant corresponding to a spherical inclusion, that is,

$$\gamma_*(x,y,z) = \begin{cases} 2, & (x-0.5)^2+(y-0.5)^2+(z-0.5)^2 \le 0.4, \\ 1, & \text{else.} \end{cases}$$

Slices of the three-dimensional reconstruction are shown in Figures 7–11.

6. Conclusions. In this work we studied issues of stability and reconstruction of the anisotropic conductivity σ of a biological medium $\Omega \subset \mathbb{R}^3$ by the hybrid inverse problem of magneto-acoustic tomography with magnetic induction (MAT-MI). More specifically, we considered a class of conductivities which correspond to a one-parameter family of symmetric and uniformly positive matrix-valued functions $t \mapsto A(x,t)$, which are a priori known to depend nonlinearly on $t \in [\lambda^{-1},\lambda]$. This gives rise to the family of anisotropic conductivities $A(x,\gamma(x))$, $x \in \Omega$, for which the goal is to stably reconstruct the scalar function γ in Ω.

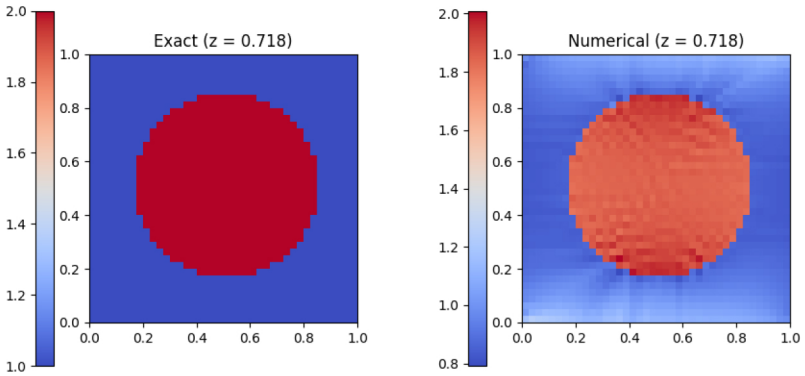

Figure 10. *Reconstruction for* (5.12) *at* $z = 0.718$.

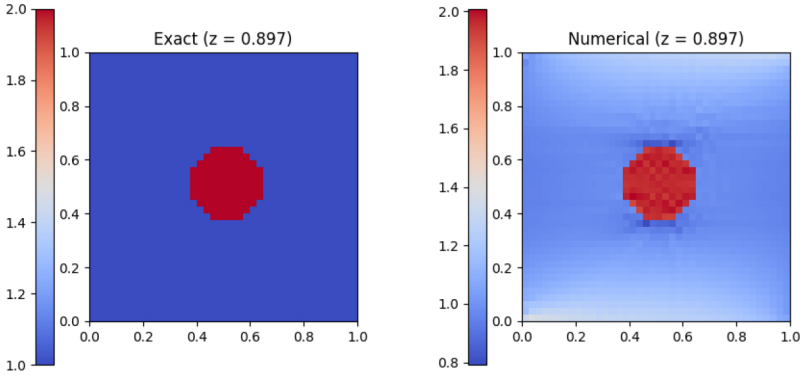

Figure 11. *Reconstruction for* A *given by the* z*-dependent* (5.12) *for* $z = 0.897$. *Ran for* 10 *iterations on a mesh of size* $40 \times 40 \times 40$.

We showed that if A belongs to certain classes of admissible anisotropic structures, then a Lipschitz type stability estimate of the scalar function in terms of the data (internal functional) holds true. In particular, the argument for our theoretical framework requires that γ and A belong to $C^{1,\beta}$. Our stability estimates extend the results in [8] to the case where σ depends nonlinearly on γ, hence allowing us to consider a more general type of anisotropic structures. Furthermore, we showed that the convergence of the reconstruction algorithm introduced in [8] extends to this nonlinear case, and demonstrated its effectiveness in several numerical experiments also showing that the reconstructions were stable in the presence of noise.

Several questions remain, including, as mentioned in [8], the reconstruction of full anisotropy, which we expect will require more measurements at hand. It will also be interesting to investigate more precisely to what extent the regularity assumptions considered in this paper are needed for the convergence of the reconstruction algorithm in practice. These questions are the subject of future work.

REFERENCES

[1] G. Alessandrini, *Singular solutions of elliptic equations and the determination of conductivity by boundary measurements*, J. Differential Equations, 84 (1990), pp. 252–272.

[2] G. Alessandrini and E. Cabib, *Determining the anisotropic traction state in a membrane by boundary measurements*, Inverse Probl. Imaging, 1 (2007), pp. 437–442.

[3] G. Alessandrini, M. De Hoop, and R. Gaburro, *Uniqueness for the electrostatic inverse boundary value problem with piecewise constant anisotropic conductivities*, Inverse Problems, 33 (2018), 125013.

[4] G. Alessandrini, M. V. de Hoop, R. Gaburro, and E. Sincich, *EIT in a layered anisotropic medium*, Inverse Probl. Imaging, 12 (2018), pp. 667–676.

[5] G. Alessandrini and R. Gaburro, *Determining conductivity with special anisotropy by boundary measurements*, SIAM J. Math. Anal., 33 (2001), pp. 153–171, https://doi.org/10.1137/S0036141000369563.

[6] G. Alessandrini and R. Gaburro, *The local Calderón problem and the determination at the boundary of the conductivity*, Comm. Partial Differential Equations, 34 (2009), pp. 918–936.

[7] H. Ammari, *An Introduction to Mathematics of Emerging Biomedical Imaging*, Math. Appl. (Berlin) 62, Springer, Berlin, 2008.

[8] H. Ammari, L. Qiu, F. Santosa, and W. Zhang, *Determining anisotropic conductivity using diffusion tensor imaging data in magneto-acoustic tomography with magnetic induction*, Inverse Problems, 33 (2017), 125006.

[9] S. R. Arridge, *Optical tomography in medical imaging*, Inverse Problems, 15 (1999), R41.

[10] K. Astala, M. Lassas, and L. Päivärinta, *Calderón inverse problem for anisotropic conductivity in the plane*, Comm. Partial Differential Equations, 30 (2005), pp. 207–224.

[11] G. Bal, *Hybrid inverse problems and internal functionals*, in Inverse Problems and Applications: Inside Out. II, Math. Sci. Res. Inst. Publ. 60, Cambridge University Press, Cambridge, UK, 2013, pp. 325–368.

[12] M. I. Belishev, *The Calderón problem for two-dimensional manifolds by the BC-method*, SIAM J. Math. Anal., 35 (2003), pp. 172–182, https://doi.org/10.1137/S0036141002413919.

[13] L. Borcea, *Electrical impedance tomography*, Inverse Problems, 18 (2002), pp. R99–R136.

[14] S. C. Brenner and L. R. Scott, *The Mathematical Theory of Finite Element Methods*, 3rd ed., Texts in Appl. Math. 15, Springer, 2007.

[15] D. C. Barber and B. H. Brown, *Applied potential tomography*, J. Phys. E. Sci. Instrum., 17 (1984), pp. 723–733.

[16] A. P. Calderón, *On an inverse boundary value problem*, in Seminar on Numerical Analysis and its Applications to Continuum Physics (Rio de Janeiro, 1980), pp. 65–73, Soc. Brasil. Mat., Rio de Janeiro, 1980; reprinted in Comput. Appl. Math., 25 (2006), pp. 133–138.

[17] W. Craggs, *Applied mathematical sciences*, Math. Gazette, 57 (1973), pp. 80–81.

[18] S. Foschiatti, R. Gaburro, and E. Sincich, *Stability for the Calderón's problem for a class of anisotropic conductivities via an ad hoc misfit functional*, Inverse Problems, 37 (2021), 125007.

[19] R. Gaburro and W. R. B. Lionheart, *Recovering Riemannian metrics in monotone families from boundary data*, Inverse Problems, 25 (2009), 045004.

[20] R. Gaburro and E. Sincich, *Lipschitz stability for the inverse conductivity problem for a conformal class of anisotropic conductivities*, Inverse Problems, 31 (2015), 015008.

[21] A. Greenleaf, M. Lassas, and G. Uhlmann, *Anisotropic conductivities that cannot be detected by EIT*, Physiol. Meas., 24 (2003), pp. 413–419.

[22] D. Gilbarg and N. Trudinger, *Elliptic Partial Differential Equations of Second Order*, The Mathematical Gazette, Springer, 1998.

[23] P. Grisvard, *Elliptic Problems in Nonsmooth Domains*, Pitman Advanced Publishing, Boston, 1985.

[24] D. Holder, *Electrical Impedance Tomography*, Institute of Physics Publishing, Bristol, 2005.

[25] D. Isaacson, J. C. Newell, J. C. Goble, and M. Cheney, *Thoracic impedance images during ventilation*, in Proceedings of the Twelfth Annual International Conference of the IEEE Engineering in Medicine and Biology Society, Philadelphia, 1990, pp. 106–107.

[26] D. Isaacson, J. Mueller, and S. Siltanen, *Biomedical applications of electrical impedance tomography*, Physiol. Meas., 24 (2003), pp. 391–638.

[27] J. Jossinet, *The impedivity of freshly excised human breast tissue*, Physiol. Meas., 19 (1998), pp. 61–75.
[28] R. Kohn and M. Vogelius, *Identification of an unknown conductivity by means of measurements at the boundary*, in Inverse Problems, SIAM-AMS Proc. 14, AMS, Providence, RI, 1984, pp. 113–123.
[29] P. Kuchment, *Mathematics of hybrid imaging: A brief review*, in The Mathematical Legacy of Leon Ehrenpreis, Springer Proc. Math. 16, Springer, Milan, 2012, pp. 183–208.
[30] L. Mariappan, G. Hu, and B. He, *Magnetoacoustic tomography with magnetic induction for high-resolution bioimepedance imaging through vector source reconstruction under the static field of MRI magnet*, Med. Phys., 41 (2014), 022902.
[31] O. G. Martinsen, S. Grimnes, and H. P. Schwan, *Interface phenomena and dielectric properties of biological tissue*, Encyclopedia Surface Colloid Sci., 7 (2002), pp. 2643–2652.
[32] R. Langer, *An inverse problem in differential equations*, Bull. Amer. Math. Soc., 39 (1933), pp. 814–820.
[33] M. Lassas and G. Uhlmann, *On determining a Riemannian manifold from the Dirichlet-to-Neumann map*, Ann. Sci. École Norm. Sup., 34 (2001), pp. 771–787.
[34] M. Lassas, G. Uhlmann, and M. Taylor, *The Dirichlet-to-Neumann map for complete Riemannian manifolds with boundary*, Comm. Anal. Geom., 11 (2003), pp. 207–221.
[35] J. M. Lee and G. Uhlmann, *Determining anisotropic real-analytic conductivities by boundary measurements*, Comm. Pure Appl. Math., 42 (1989), pp. 1097–1112.
[36] W. R. B. Lionheart, *Conformal uniqueness results in anisotropic electrical impedance imaging*, Inverse Problems, 13 (1997), pp. 125–134.
[37] L. Qiu and F. Santosa, *Analysis of the magnetoacoustic tomography with magnetic induction*, SIAM J. Imaging Sci., 8 (2015), pp. 2070–2086, https://doi.org/10.1137/15M1012323.
[38] L. B. Slitchter, *An inverse boundary value problem in electrodynamics*, Physics, 4 (1933), pp. 411–418.
[39] J. Sylvester, *An anisotropic inverse boundary value problem*, Comm. Pure. Appl. Math., 43 (1990), pp. 201–232.
[40] A. N. Tikhonov, *Uniqueness of the solution for the problem of electrical prospecting*, Dokl. Akad. Nauk SSSR, 69 (1949), pp. 780–797.
[41] G. Uhlmann, *Electrical impedance tomography and Calderón's problem (topical review)*, Inverse Problems, 25 (2009), 123011, https://doi.org/10.1088/0266-5611/25/12/123011.
[42] T. Widlak and O. Scherzer, *Hybrid tomography for conductivity imaging*, Inverse Problems, 28 (2012), 084008.
[43] Y. Xu and B. He, *Magnetoacoustic tomography with magnetic induction (MAT-MI)*, Phys. Med. Biol., 50 (2005), pp. 5175–5187.
[44] Y. Zou and Z. Guo, *A review of electrical impedance techniques for breast cancer detection*, Med Eng. Phys., 25 (2003), pp. 79–90.